Available online at www.sciencedirect.com
SCIENCE DIRECT
Journal of Solid State Chemistry 179 (2006) 2547–2553
JOURNAL OF SOLID STATE CHEMISTRY
www.elsevier.com/locate/jssc

Preparation and formation mechanism of wood-block-like calcite particles

Hua Guo, Jiaguo Yu*, Bei Cheng

State Key Laboratory of Advanced Technology for Material Synthesis and Processing, Wuhan University of Technology, Wuhan 430070, PR China

Received 19 November 2005; received in revised form 12 January 2006; accepted 8 May 2006
Available online 13 May 2006

Abstract

Pure calcite crystal with different morphologies such as wood-block and spherical aggregates were prepared by a precipitation reaction in the presence of citric acid. The as-prepared products were characterized with scanning electron microscope (SEM) and X-ray diffraction (XRD). The results showed that citric acid obviously influenced the formation of precipitates and the morphology of final products. The formation mechanism of wood-block-like particles was proposed according to theoretical deduction and the proposed growth mode.

Keywords: Calcite; Citric acid; Wood-block-like particle; Stereo structure; Theoretical deduction; Precipitation mechanism; Growth mode

1. Introduction

The crystallization of calcium carbonate in an aqueous solution is a problem attracting the attention of many investigators in a variety of fields, such as geochemistry, biomineralization and chemical engineering because calcium carbonate is encountered in innumerable situations both in industry and in the natural environment [1–4]. The morphology and polymorph of calcium carbonate are highly sensitive to the local conditions of precipitation, temperature, supersaturation, pH values, molar ratio of reactants, and the presence of additives and impurities, etc [5–8]. The type of polar functional groups contained in the additives [9], the number of polar functional groups per molecule [10–13], hydrophobic and hydrophilic regions [14], the molecular weight and the concentration of additives [15], and a match between the spacings of functional groups and the spacings of cations on crystal surface [16] are considered to be the most important factors that influence crystallization. It is proposed that the additives have two functions: (a) a heterogeneous nucleator and (b) an inhibitor for crystal growth by binding to the growth sites of the crystals [10].

In recent years, much research work has been conducted in laboratories to mimic the biosynthesis of calcium carbonate [17–23], but breakthrough progresses on quantitatively understanding the role of additives were limited. It was found that carboxylate groups had obvious influences on the morphology and crystallization of inorganic minerals. So it was reasonable to believe that simple carboxylic acid with small molecular weight would effectively influence the crystallization of calcium carbonate under proper experimental conditions.

In this work, citric acid was used as an additive to control the nucleation and growth of calcium carbonate, and different morphological calcium carbonate particles such as wood-block and spherical aggregates were obtained. We simulated the stereo structures of ionized citric acid and studied the surface properties of crystal faces of calcite carbonate by using the softwares "ChemSketch" and "Materials Studio". How the carboxylate groups of ionized citric acid were attracted on the growth sites of calcite crystal and the reason why different morphological calcium carbonate particles were formed in the presence of citric acid were analyzed in details. This work may provide new insight into the comprehension on

*Corresponding author. Fax: +86 27 8788 2395.
E-mail address: jiaguoyu@yahoo.com (J. Yu).

0022-4596/$ - see front matter © 2006 Elsevier Inc. All rights reserved.
doi:10.1016/j.jssc.2006.05.005

the interaction between the organic additives and calcium carbonates.

2. Experimental section

2.1. Preparation

Unless otherwise stated, all chemicals used in the experiments were of analytical grade, and the water used in this work was distilled water. The preparations of calcium carbonate were carried out in glass beakers at room temperature (ca. 25 °C). Aqueous solutions of Na_2CO_3 (0.5 M), $CaCl_2$ (0.5 M) and citric acid (0.2 M) were first prepared as stock solutions. In a typical synthesis, a given amount of citric acid solution was added into 96 mL distilled water and the pH of the as-obtained solution was adjusted to a desired pH value (e.g., pH 10) by using 1.0 M HCl or 1.0 M NaOH solution. Then a solution of $CaCl_2$ (0.5 M, 1 mL) was injected into the above pH-adjusted solution. Finally, a solution of Na_2CO_3 (0.5 M, 1 mL) was quickly injected into the mixed solution under vigorous stirring by using a magnetic stirrer. This gave a final $CaCO_3$ concentration of 5 mM. The mixture was stirred for 1 min, and then the beaker was covered and allowed to stand under static conditions for 24 h. In the experiments, the final concentration of citric acid was varied from 0.4 to 8 mM and all the other conditions were kept the same. The obtained products were centrifuged and washed with distilled water and absolute ethanol for three times, respectively, and then dried in a vacuum oven at 60 °C before they were collected for characterization.

2.2. Characterization

The as-prepared $CaCO_3$ precipitations were characterized by scanning electron microscope (SEM) (type: JSM-5610, Japan) with an accelerating voltage of 20 kV. The powder XRD patterns were obtained on a HZG41B-PC X-ray diffractometer using Cu $K\alpha$ radiation at a scan rate of 0.05° $2\theta\,S^{-1}$. The accelerating voltage and the applied current were 15 kV and 20 mA, respectively.

3. Results and discussion

3.1. XRD patterns and SEM images

The XRD patterns of the as-prepared $CaCO_3$ products in the presence of citric acid are shown in Fig. 1. All the diffraction peaks can be readily indexed to calcite polymorph of $CaCO_3$ [space group: $R\bar{3}c$ (167)] with a lattice constant $a = 4.988$ and $c = 17.05$ Å (JCPDS 83-1762). The strong and sharp peaks indicate that the samples are well crystallized. No obvious characteristic diffraction peaks of any impurities can be detected. It can be found from Fig. 1 that with increasing the concentration of citric acid, the diffraction intensities of {110} and {100} faces increase (as shown in Fig. 1(b) and (c)). On the contrary, the relative

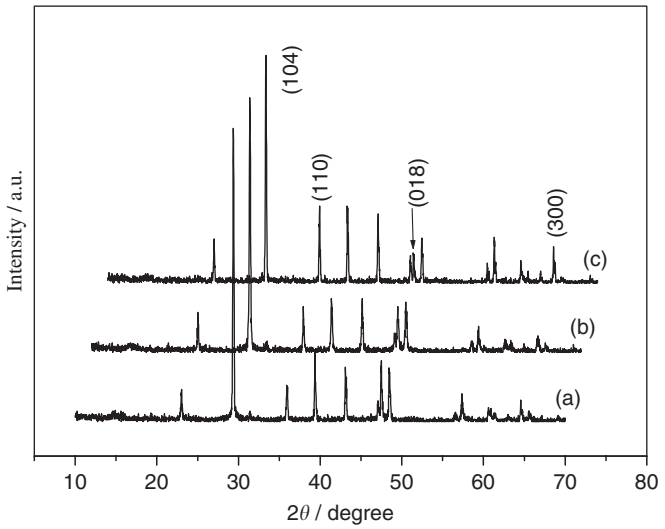

Fig. 1. XRD patterns of $CaCO_3$ powders obtained in the presence of 0.4 (a), 4 (b) and 8 mM (c) citric acid.

intensity of {104} faces slightly decreases. This indicates that the growth rate of {100} and {110} faces decreases with increasing the concentration of citric acid. This results in a good crystallization or greater exposition of {*hk*0} faces. All these results indicate that these samples exhibit different growth tropisms in the presence of citric acid.

Fig. 2 shows SEM images of $CaCO_3$ powders obtained in the absence and presence of citric acid. It can be seen that the presence of citric acid obviously influence the morphology of the as-prepared calcium carbonate particles. The particles obtained in pure water are rhombohedral calcite crystals (Fig. 2(a)). The inset image is an amplified calcite rhombohedron. When a small amount of citric acid (0.4 mM) was added, the morphology of $CaCO_3$ particles was changed from rhombohedron to spherical aggregates (as shown in Fig. 2(b)). It can be seen from Fig. 2(b) that these spherical aggregated particles are composed of many small crystals. An amplified image (see Fig. 2(c)) clearly reveals such a superstructure. When the concentration of citric acid reaches 2.6 mM, the morphology of the as-obtained $CaCO_3$ particles is still spherical aggregates (as shown in Fig. 2(d) and 2(e)). It can be seen from Fig. 2(e) and (c) that the $CaCO_3$ particles obtained at [citric acid] = 2.6 mM consists of smaller crystals. This is due to the fact that more ionized citric acid inhibits the growth of $CaCO_3$ particles.

At [citric acid] = 4 mM, two distinctive morphologies are observed (as shown in Fig. 2(f)). One is quasi-spherical aggregated particles. The other looks like rice. An amplified image (the inset in Fig. 2(f)) reveals that these novel rice-like particles are covered by rhombohedral {104} faces at both ends [5] and the edges of these crystal faces are not very sharp. Generally speaking, the faster a crystal face grows, the weaker the crystallization will be. Hence, it will be reasonable to conclude that the formation of such {104} crystal faces is due to their relatively fast growth rate.

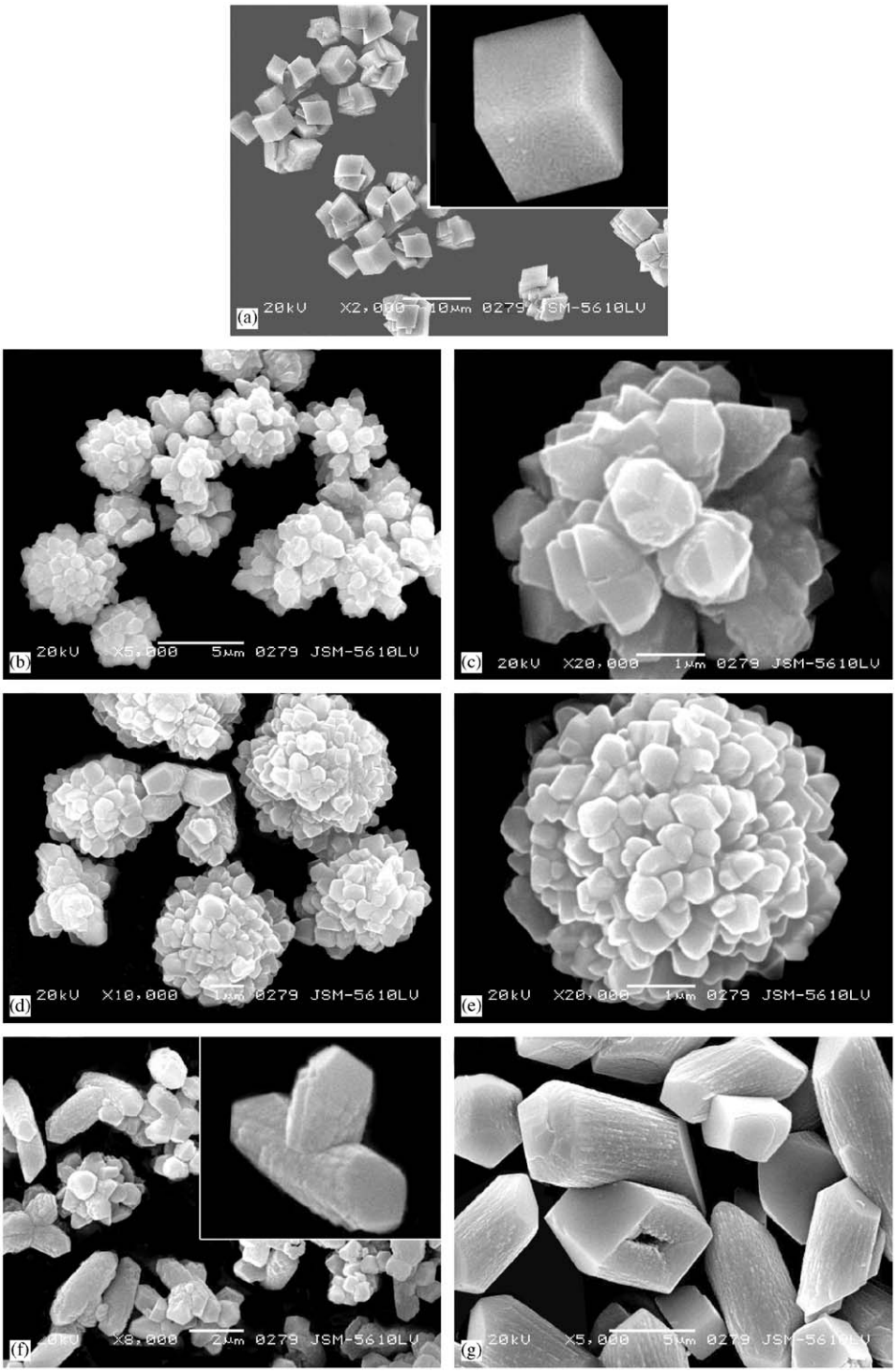

Fig. 2. SEM images of $CaCO_3$ powders obtained in the presence of 0 (a), 0.4 (b and c), 2.6 (d and e), 4 (f) and 8 mM (g) citric acid.

When the concentration of citric acid was further increased to 8 mM, the spherical aggregated particles completely disappeared. The as-prepared samples almost were uniform wood-block-like particles (Fig. 2(g)). Such morphologies are constituted with cylindrical side surfaces and several sets of coupled {104} crystal faces at both ends. It can also be observed from Fig. 2(g) that the textures of the side surfaces are highly ordered. This indicates that the formation of the texture should have some relationship with the inner crystalline structure. The formation of such wood-block-like morphology indicates that the crystals grow at a low nucleation and growth rate. This also agreed with the observed precipitating phenomena. It is interesting to note that the concentration of citric acid obviously influences the rate of precipitate formation. If the concentration of citric acid is much lower than 4 mM, such as 0.4 or 2.6 mM,

the reaction solution become turbid immediately after Na_2CO_3 solution was added into $CaCl_2$ solution. At [citric acid] = 4 mM, the mixed solution of Na_2CO_3 and $CaCl_2$ appears semi-transparent. When the concentration of citric acid reaches 8 mM, the mixed solution keeps transparent for a long time. The precipitates cannot be observed until several hours later. These experimental results indicate that the concentrations of citric acid significantly influence the nucleation and growth rate of calcite crystals. According to the precipitating phenomenon and the SEM observations (especially Fig. 2f), it will be reasonable to believe that [citric acid] at 4 mM should be an intermediate concentration, which indicates the transformation of the morphologies from spherical aggregates to wood-block-like single crystal particles.

3.2. Mechanism discussion

3.2.1. Formation mechanism of wood-block-like particles

Although similar wood-block-like particles were also prepared by Albeck et al. [5] in the presence of macromolecules, no formation mechanism and theoretical explanation were reported. We believe that under given conditions, calcite rhombohedron can elongate along some crystallographic axis (such as *c*-axis) if only the crystal faces parallel to the *c*-axis (such as {100} and {110}) grow at a rate much lower than that of *c*-axial direction. Such a growth mode can be realized through selective adsorption of ionized citric acid on these crystal faces. Therefore, we speculate that these wood-block-like particles are the deformations of calcite rhombohedra.

It has been demonstrated that some short-chain additives can interact specifically with two different Ca^{2+} ions exposed on crystal faces of calcite if the spacing of two carboxylate groups is close to 0.4 nm [16]. If the distance of two neighboring carboxylate groups can match the spacing between two different Ca^{2+} ions exposed on a given crystal face, the above-mentioned competitive growth mode will be easily realized. Hence, we calculate face parameters of calcite crystal using the software "Materials Studio" and corresponding distances of carboxylate groups of ionized citric acid structures using the software "ChemSketch". The simulated results are shown in Table 1 and Fig. 3, respectively. It can be seen from Table 1 that {104}, {110} and {100} faces contain Ca^{2+} ions with spacing distances about 4.990 Å and/or 4.048 Å. Fig. 3 reveals that carboxylate groups of ionized citric acid have several different distances, among which there exist two sets of meaningful distances, i.e., ca. 5 and 4 Å. The two sets of distances can perfectly match the Ca^{2+} ions with spacings of 4.990 and 4.048 Å, respectively. From the above discussion and the data shown in Table 1, we believe that ionized citric acid can simultaneously adsorb on {104}, {100} and {110} faces and the relative adsorption amount of the ionized citric acid on these faces determine their growth rates. This has been demonstrated by the XRD results. Table 1 also shows that {104}, {100} and {110} crystal faces all are neutral-charged faces, which have relatively low surface energy. This makes them possible to become habit faces. It can be seen from Table 1 that, besides {104}, {110} and {100} crystal faces, there exist other sets of crystal faces (such as {012}, {006} and {202}, etc.), which contain Ca^{2+} with distance matching the spacing of functional carboxylate groups. But from the column of charge property in Table 1, it can be found that all these crystal faces are imbalance-charged faces except for {018} faces. Such face structure determines that these crystal faces have relative high surface energy contrasted with those neutral-charged crystal faces. So the adsorptive effect of ionized citric acid may be weakened due to the relative high growth rates of these faces. This can account for the reason why only {104}, {110} and {100} were obviously influenced in this study. The exceptional character of neutral-charged {018} crystal face may be due to the fact that the tilted carbonate

Table 1
Face parameters of calcite crystal simulated and calculated by using "Materials Studio"

Crystal faces	Interplanar[a] spacing (Å)	Charge property of the layer	Spacing of two neighboring Ca^{2+} ions on each layer (Å)
(104)	**3.0355**	**Neutral**[b]	**4.048; 4.990**
(110)	**2.4948**	**Neutral**	**4.048; 6.375**
(300)	**1.4403**	**Neutral**	**4.990**
(012)	3.8547	Alternate[c]	4.048; 4.990; 6.375
(006)	2.8435	Alternate	4.990; 4.990; 4.990
(113)	2.2846	Imbalanced[d]	6.375; 8.463
(202)	2.0944	Imbalanced	4.990; 6.375
(024)	1.9273	Alternate	4.048; 4.990
(018)	1.9124	Neutral	4.990
(116)	1.8753	Imbalanced	4.048; 8.643
(211)	1.6258	Imbalanced	6.375; 11.842
(122)	1.6040	Imbalanced	4.048; 9.510
(214)	1.5252	Neutral	6.375

[a]Interplanar spacing was excerpted from standard XRD pattern of calcite.
[b]The number of Ca^{2+} equals to the number of CO_3^{2-} in one {*hkl*} plane.
[c]A {*hkl*} plane containing only Ca^{2+} or CO_3^{2-} ions alternately appears at regular distance.
[d]Ca^{2+} and CO_3^{2-} cannot be contained simultaneously in one {*hkl*} plane.

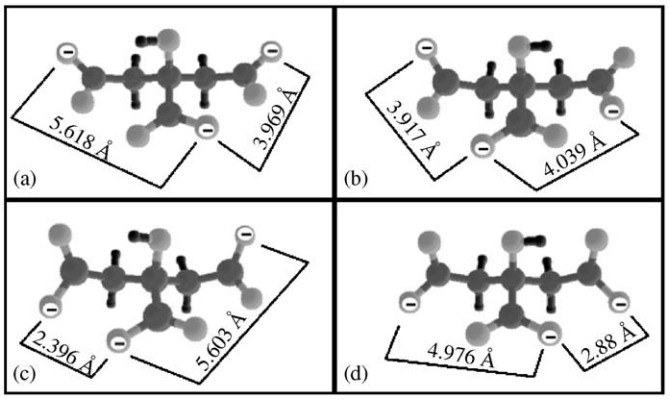

Fig. 3. Several representative stereo structures of ionized citric acid simulated by using the software "ChemSketch".

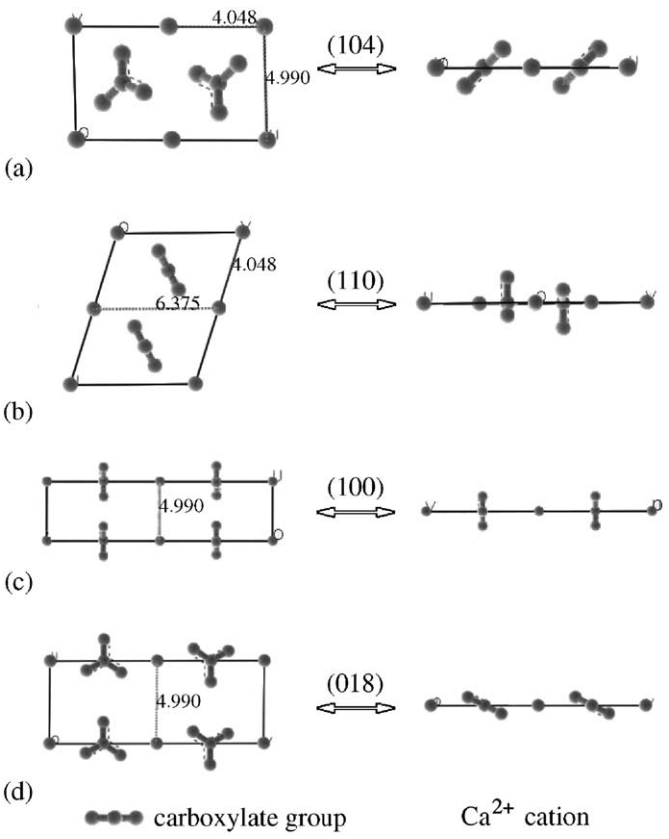

Fig. 4. Simulated neutral-charged crystal planes of calcite carbonate by "Materials Studio".

groups with a large angle (as shown in Fig. 4d) seriously inhibit ionized citric acid to interact with Ca^{2+} cations. Hence, ionized citric acid had a small influence on the growth of {018} crystal face, which resulted in a slight decrease in the intensity of {018} X-ray diffraction peak (as shown in Fig. 1).

It has been widely accepted in classical theories for crystal growth that (a) crystal polyhedra grown by a layer-by-layer mechanism at moderate supersaturation and (b) the growth rate of the given face is proportional to the distance between the face and the center of equilibrium polyhedron [16,24]. Based on the above theory, several probable equilibrium morphologies of calcite can be deduced if a calcite rhombohedron is a competitive result of {104}, {100} and {110} faces. Fig. 5(a) and (b) show the Miller indexes of crystal faces on a perfect calcite rhombohedron. Fig. 5(c) is a combined figure, which shows the relative distances of crystal faces on a perfect calcite rhombohedron (simulated in "Materials Studio"). The relative growth rates, R_1, R_2 and R_3, are defined as

$$R_1 = d_{\{104\}}/d_{\{100\}},$$

$$R_2 = d_{\{104\}}/d_{\{110\}},$$

$$R_3 = d_{\{100\}}/d_{\{110\}}.$$

(A) The detailed deduction process has not been given here. $R_1 = (17/32.5) = 0.523$, $R_2 = (17/28) = 0.607$; a perfect calcite rhombohedron can be obtained.
(B) $R_2 = 0.607$, $R_3 = (\sqrt{3}/2)$; the growth rate of {100} faces is lower than that of {110} faces and {100} faces will be exposed gradually.
(C) $R_2 > 0.607$, $R_3 = (\sqrt{3}/2)$; the polyhedron formed in (C) will be elongated along the c-axis.
(D) $R_1 = 0.523$, $R_3 = \sqrt{3}$; the growth rate of {110} faces is lower than that of {100} faces and {110} faces will be exposed gradually.
(E) $R_1 > 0.523$, $R_3 = \sqrt{3}$; the polyhedron formed in (C) will also be elongated along c-axis.
(F) $R_2 > 0.607$, $R_1 > 0.523$, $R_3 = 1$; a rhombohedron simultaneously covered by six {104} faces, six {100} faces and six {110} faces will be formed. Under this condition:$(\sqrt{3}/2) < R_3 < 1$, {110} faces are inclined to disappear; $1 < R_3 < \sqrt{3}$, {100} faces become disappearing faces. The value of R_3 determines the disappearing rate of the two sets of faces. The larger the value deviates from 1, the faster the corresponding faces disappears.

The above discussion provides a theoretical support for the formation of elongated calcite rhombohedra according to the adsorption of ionized citric acid on these crystal faces. In addition, the formation of cylindrical side surface (as shown in Fig. 6(b)) needs one more condition: different layers of {hk0} face continue to grow, respectively. Such growth mode of {hk0} faces will insure the formation of cylindrical side surface of the elongated rhombohedron, which makes it look like wood-blocks. Moreover, such continuous growth mode will also insure the respective exposition of the layer-edges (parallel to the c-axis) (see Fig. 6(a)). To particular crystal particles, the exposition of the different layer-edges will present as an ordered texture on the side surface of particles (as shown in Fig. 7(b)).

Fig. 7(a) and (b) show direct evidences to the above-proposed growth model. The large circular inset in Fig. 7(a) is an amplified image for growth details, in which

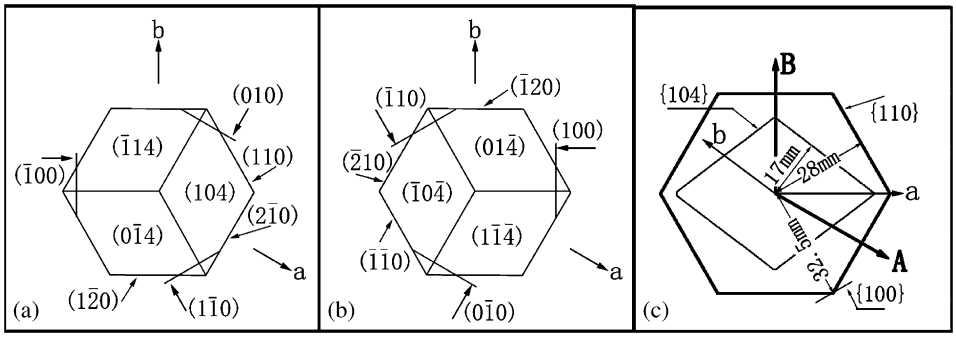

Fig. 5. Projective images (a and b) of calcite rhombohedron along the *c*-axis: (a) view along [00$\bar{1}$] direction and (b) view along [001] direction. (c) A combined projective figure to show the relative distance of crystal faces on a calcite rhombohedron. The labeled values in (c) are the measured projective lengths, instead of the real lengths of the crystal faces.

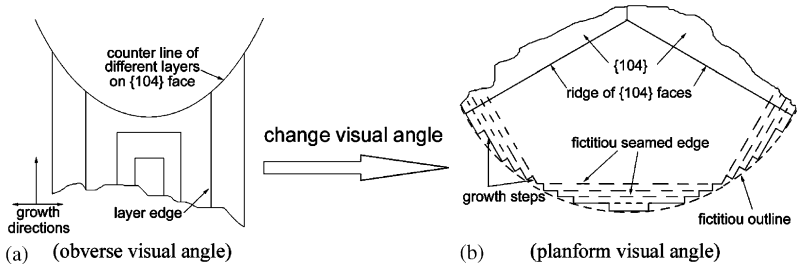

Fig. 6. Schematic model for the growth of wood-block-like particles. (a) Layer edges on different {*hk*0} layers, and (b) cylindrical side surface.

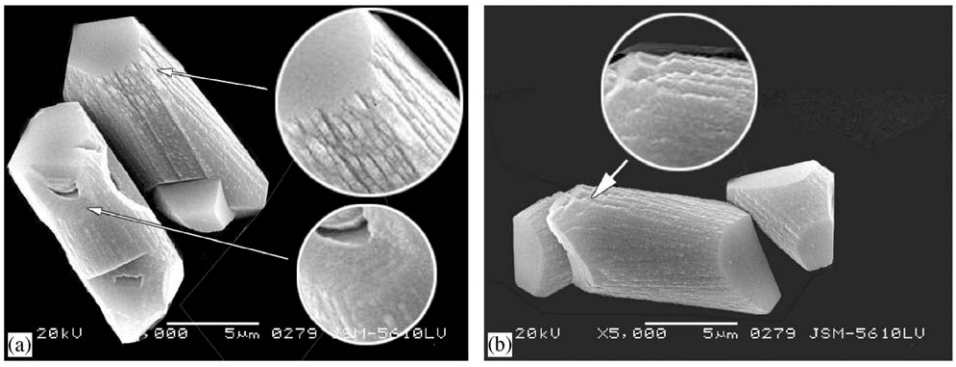

Fig. 7. SEM images of calcite particles obtained in the presence of 8 mM citric acid and corresponding amplified image.

different growth layers can be clearly distinguished. Judged from the structure of calcite crystal, these layers should belong to {100} faces. The small circular inset in Fig. 7(a) is a crystal defect, which directly proves that the ordered texture on the side surface of wood-block-like particle is the exposition of different-layer edges. The inset in Fig. 7(b) clearly reveals an enveloping mode at the ends of new layers and the steps of {104}. These observations provide powerful supports to the above mechanism. Meanwhile, two kinds of representative side-surface textures can be observed from Fig. 7(b). One texture is a set of paralleled line (the right and the left particles). The other one is a set of cross lines (the middle one). This difference may be ascribed to whether or not the crystallographic *c*-axis parallels to the particle axis. If yes, the surface texture will be a set of parallels, otherwise, it will be cross lines.

3.2.2. Formation mechanism of spherical aggregated particles

As has been mentioned above, the concentration of citric acid obviously influences the formation rate and morphology of the precipitates. At a high citric acid concentration, wood-block-like particles were formed due to a low supersaturation because most of Ca^{2+} ions were chelated by ionized citric acid and were then released slowly during

crystallization stage. On the contrary, low citric acid concentrations resulted in the formation of spherical $CaCO_3$ aggregated particles due to relative high supersaturation of reactants. It was assumed that crystal faces of the primarily formed small $CaCO_3$ crystals at this supersaturation were selectively capped by ionized citric acid. Those uncapped crystal faces attracted each other to reduce the excess surface energy, leading to the formation of lager spherical aggregates. Diffusion-control growth [25,26] then occurred in the spherical aggregates as the $CaCO_3$ crystals were in a close contact, and the surface area was reduced by the fusion of crystals and the rearrangement of structure [27–29]. Therefore, spherical $CaCO_3$ aggregated particles with a rough surface were obtained at low citric acid concentration range.

4. Conclusions

In summary, pure calcite particles with different morphologies were successfully prepared through aqueous-phased routes employing calcium chloride and sodium carbonate as the reactants and using citric acid as a crystallization modifier. The ionized citric acid showed obvious influence on the stages of nucleation and aggregation and crystal growth during the crystallization process of calcium carbonate. The concentration of citric acid obviously influenced the final morphology or aggregation mode of calcite crystals. The formation mechanisms of wood-block-like particles as well as the particles with other shapes were proposed. This research could provide important information about the interaction between organic additives and crystallization of calcium carbonate.

Acknowledgments

This work was partially supported by the National Science Foundation of China (50272049 and 20473059). This work was also financially supported by the Excellent Young Teachers Program of MOE of China and Project-Sponsored by SRF for ROCS of SEM of China, Key Project of State Key Laboratory of Advanced Technology for Materials Synthesis and Processing (WUT2004Z03).

References

[1] S. Mann, G.A. Ozin, Nature 382 (1996) 313.
[2] H. Yang, N. Coombs, G.A. Ozin, Nature 386 (1997) 692.
[3] T.S. Ahmadi, Z.L. Wang, T.C. Green, A. Henglein, M.A. El-Sayed, Science 272 (1996) 1924.
[4] D.B. Zhang, L.M. Qi, J.M. Ma, H.M. Cheng, Chem. Mater. 14 (2002) 2450.
[5] S. Albeck, J. Aizenberg, L. Addadi, S. Weiner, J. Am. Chem. Soc. 115 (1993) 11691.
[6] G. Falini, S. Albeck, S. Weiner, L. Addadi, Science 271 (1996) 67.
[7] A. Belcher, X. Wu, R. Christensen, P. Hansma, G. Stucky, D. Morse, Nature 381 (1996) 56.
[8] J.G. Yu, H. Guo, B. Cheng, J. Solid State Chem. 179 (2006) 800.
[9] J.G. Yu, X.F. Zhao, B. Cheng, Q.J. Zhang, J. Solid State Chem. 178 (2005) 861.
[10] N. Wada, K. Kanamura, T. Umegaki, J. Colloid Interface Sci. 233 (2001) 65.
[11] N. Wada, K. Yamashita, T. Umegaki, J. Colloid Interface Sci. 212 (2001) 357.
[12] K.-J. Westin, A.C. Rasmuson, J. Colloid Interface Sci. 282 (2005) 359.
[13] C. Geffroy, A. Foissy, J. Persello, B. Cabane, J. Colloid Interface Sci. 211 (1999) 45.
[14] L.M. Qi, J. Li, J.M. Ma, Adv. Mater. 14 (2002) 300.
[15] J. Donners, B.R. Heywood, E.W. Meijer, R.J.M. Nolte, C. Roman, A. Schenning, N. Sommerdijk, Chem. Commun. 19 (2000) 1937.
[16] S. Mann, Biomineralization: Principles and Concepts in Bioinorganic Materials Chemistry, Oxford University Press, Oxford, 2001.
[17] C.M. Zaremba, D.E. Morse, S. Mann, P.K. Hansma, G.D. Stucky, Chem. Mater. 10 (1998) 3813.
[18] B.R. Heywood, S. Mann, Adv. Mater. 6 (1994) 9.
[19] J. Kuther, G. Nelles, R. Seshadri, M. Schaub, H.J. Butt, W. Tremel, Chem. Eur. J. 4 (1998) 1834.
[20] C. Damle, A. Kumar, M. Bhagwat, S.R. Sainkar, M. Sastry, Langmuir 18 (2002) 6075.
[21] D. Walsh, S. Mann, Nature 377 (1995) 320.
[22] J. Aizenberg, D.A. Muller, J.L. Grazul, D.R. Hamann, Science 299 (2003) 1205.
[23] J.J.J.M. Donners, R.J.M. Nolte, N.A.J.M. Sommerdijk, J. Am. Chem. Soc. 124 (2002) 9700.
[24] S. Mann, Biomimetic Materials Chemistry, VCH Publishers, New York, 1996.
[25] X.G. Peng, L. Manna, W. Yang, J. Wickham, E. Scher, A. Kadavanish, A.P. Alivisato, Nature 404 (2000) 59.
[26] X.G. Peng, J. Wickham, A.P. Alivisatos, J. Am. Chem. Soc. 120 (1998) 5343.
[27] X.F. Zhao, J.G. Yu, B. Cheng, Q.J. Zhang, Colloid Surf. A 268 (2005) 78.
[28] S.W. Liu, J.G. Yu, B. Cheng, L. Zhao, Q.J. Zhang, J. Crystal Growth 279 (2005) 461.
[29] J.G. Yu, S.W. Liu, B. Cheng, J. Crystal Growth 275 (2005) 572.